Structural Volume Changes upon Photoisomerization: A Laser-Induced Optoacoustic Study with a Water-Soluble Nitrostilbene

Ingolf Michler, Alessandro Feis,† Miguel A. Rodríguez,‡ and Silvia E. Braslavsky*

Max-Planck-Institut für Strahlenchemie, Postfach 10 13 65, D-45413 Mülheim an der Ruhr, Germany

Received: November 30, 2000; In Final Form: February 22, 2001

The *trans* to *cis* photoisomerization of 4,4′-dinitro-2,2′-disulfonylstilbene (DS) was studied by laser-induced optoacoustic spectroscopy (LIOAS) in aereated neat water and in aereated aqueous solutions of various monovalent cations (NH_4^+, $N(CH_3)_4^+$, Na^+, K^+, and Cs^+) and the respective *cis* to *trans* photoisomerization only in the presence of NH_4^+. In every case, two single-exponential components were required to fit the data, one with an unresolved lifetime (<20 ns) for the appearance of the triplet state mixture T (the perpendicular triplet state ^{3}p* in equilibrium with the lowest *trans* triplet state ^{3}t*) and one with a longer lifetime of (75 ± 20) ns at 5.5 °C for the decay of the T mixture. The temperature dependence of the LIOAS amplitudes in combination with the determined isomerization quantum yields afforded a contraction of −(1.4 ± 0.15) ml/mol for the *trans* to T transition, whereas a smaller contraction of −(0.15 ± 0.15) ml/mol was obtained for the *cis* to T transition. The different values of the contraction indicate a greater similarity between the average structures of the T components with the *cis* ground singlet state than with the *trans* ground singlet. The total structural volume change for the *trans* to *cis* transition is in average $\Delta V_{tc} = -(1.2 \pm 0.1)$ ml/mol. The calculated contribution of electrostriction is at most 50% of this value. However, the nature of the countercation had no influence on the data as would be expected for changes in the specific interaction with the H-bond network in water upon photoisomerization. Thus, ca. 50% of the total contraction is attributed to intrinsic effects, related to a shorter C═C bond and a smaller accessible volume in the *cis* isomer. The LIOAS data show that *cis*-DS lies (28 ± 35) kJ/mol above *trans*-DS in agreement with the calculated value of 37 kJ/mol.

Introduction

Measurements of reaction volume changes during isomerization reactions by conventional techniques (i.e., by analyzing the pressure dependence of the equilibrium constant) are infrequent.[1] One of the reasons is probably the small expected value of ΔV_R. Another reason is that in order to obtain ΔV_R from steady-state measurements, relatively large pressure variations are needed, which poses special technical problems for photoreactions. Laser-induced optoacoustic spectroscopy (LIOAS)[2] is thus the method of choice for the determination of those volume changes.

During our LIOAS study with 3,3′-diethyloxadicarbocyanine iodide (DODCI), we concluded that the photoinduced structural volume changes in aqueous solutions are mainly due to changes in the specific interactions of the solvent molecules with the isomerized DODCI.[3] The contraction of $\Delta V_R = -29$ mL/mol upon *trans* → *cis* isomerization cannot be explained with the continuum model for electrostriction, originally used by Drude and Nernst[4] to relate the reorganization of solvent around solvated ions. The calculated[5] electrostrictive contraction of ca. 0.1 ml/mol is negligible in comparison to the effect observed which, therefore, should be attributed to changes in the hydrogen bond strength between the solvent molecules and the photoisomer versus the parent compound. Most probably, the lone pair of one of the heterocyclic nitrogens is involved in these hydrogen bonds.[3]

The contractions determined by LIOAS for the *trans* → *cis* photoisomerization of the three isomers (*para*, *meta*, and *ortho*) of potassium azobenzenecarboxylates were also rationalized in terms of the difference in the chromophore−water hydrogen bonds strength between the photoisomer and the parent compound. Due to a reduced conjugation, a stronger interaction of the nitrogens' lone pairs and water is expected in the *cis* isomers, leading to the contraction upon photoisomerization.[6]

On the contrary, the values of ΔV_R observed for intramolecular electron-transfer reactions of large donor−bridge−acceptor molecules in nonpolar organic solvents can be indeed explained by using the concept of a solvent continuum, in addition to intrinsic photoinduced changes, such as intramolecular exciplex formation (a transient isomerization) in flexible donor−bridge−acceptor molecules.[7,8] Intrinsic volume changes explain also the contraction measured upon photoexcitation of $Ru(bpy)_3^{2+}$ (unable to form hydrogen bonds) in water in view of the shortening of the Ru−N bond in the produced metal-to-ligand charge transfer state.[9]

Thus, a picture emerges which relates the photoinduced structural volume changes to the particular type of chromophore-medium interactions. We are interested in finding a general picture relating the structural volume changes to molecular properties that would help us understanding the changes observed upon photoexcitation of biological photosensors.[10−12]

To this aim, we performed LIOAS studies of three retinal isomers in a series of *n*-alkanes. These studies helped us to understand the different photochemistry of the isomers but little could be learned about the time-resolved ΔV_R values.[13] The low photoisomerization quantum yield for all-*trans*-retinal and a

* To whom correspondence should be addressed. E-mail: braslavskys@mpi-muelheim.mpg.de. Fax: *49 (208) 306 3951.

† Present address: Dipartimento di Chimica, Universitá di Firenze, Via Gino Capponi 9, I-50121 Firenze, Italy.

‡ On leave from the Departamento de Química, Universidad de La Rioja, E−26071 Logroño, Spain.

10.1021/jp004334m CCC: $20.00
Published on Web 04/25/2001

dependence of the isomerization quantum yield on the solvent for 13-*cis*-retinal difficulted the quantitative evaluations.

We thus decided to determine by LIOAS the ΔV_R values for the photoisomerization of a water-soluble stilbene derivative, 4,4′-dinitro-2,2′-disulfonylstilbene (DS) because the *cis* → *trans* transformation of stilbene and its derivatives is one of the most investigated photoisomerizations, the energetics and dynamics of these systems have been extensively characterized, and the isomerization quantum yields are in general large.[14,15]

An advantage of DS is that the *cis* and *trans* isomers are separable and stable in their ground states. Thus, a reaction volume change determination is possible for the photoisomerization in both directions.

In the present paper, we concentrate on the structural volume changes derived from LIOAS studies for the *trans* → *cis* and *cis* → *trans* photoisomerization of DS in neat water and in aqueous solutions of various monovalent cations.

An adequate knowledge of the photochemical properties is a prerequisite for the determination of ΔV_R by LIOAS. To this aim, we measured the photoisomerization and fluorescence quantum yields of both DS isomers and checked for the presence of long-lived energy-storing species upon photoexcitation of both isomers. To estimate the electrostriction volume change we also calculated the variation in dipole moment upon photoisomerization and the size of each isomer.

Materials and Methods

Protonated 4,4′-dinitro-2,2′-disulfonylstilbene (DS) in its *trans*-isomeric form (Bayer) was recrystallized twice from methanol−water.

To obtain *cis*-DS a 0.17 M solution of *trans*-DS in the HPLC mobile phase (vide infra) was irradiated for 10 min with a 250-W tungsten halogen lamp. The photoisomer mixture of *trans*- and *cis*-DS was separated on a preparative reversed phase HPLC column (Nucleosil-C18−120−3) with a 0.07 M NH_4-CH_3COO in 20% CH_3CN/H_2O solution. After separation, CH_3-CN was evaporated.

All measurements with the *cis*-DS were performed in aqueous 90 mM NH_4CH_3COO solutions. The *trans*-DS was investigated in aqueous solutions containing 90 mM acetate salts of one of the monovalent cations NH_4^+, $N(CH_3)_4^+$, Na^+, K^+, and Cs^+, as well as in neat water. Water was tri-distilled. $K_2Cr_2O_7$ (Merck) and indigocarmin (EGA-Chemie, Steinheim/Albuch, Germany) were the calorimetric reference substances, the former for the monovalent salt solutions and the latter for neat water. $K_2Cr_2O_7$ was not stable in neat water. 5,10,15,20-Tetrakis-(4-sulfonatophenyl)-porphyrin (TSPP, Porphyrin Products Inc.) in tris buffer (pH = 7.8) was used as a standard photosensitizer for the generation of molecular singlet oxygen, $O_2(^1\Delta_g)$. $K_2Cr_2O_7$, indigocarmin, and TSPP were used without further purification.

In every case, the samples as well as the reference solutions were stirred in order to minimize the build up of the respective other isomer in the excited volume.

Absorption Measurements. Absorption measurements were carried out with a Shimadzu UV-2102PC spectrophotometer. The sample and reference solutions were matched in absorbance within 5% at the excitation wavelength for the LIOAS experiments. In the first measurements series, absorbances in the range of $A^{355} = 0.1-0.3$ were used (2 ml sample volume), whereas an (initial) absorbance of $A^{355} = 0.3$ (3 ml sample volume) was kept for all experiments throughout the second and third series. Absorption spectra were recorded between 200 and 500 nm for the determination of the isomerization quantum yields.

LIOAS. LIOAS was performed as already described using the 3rd harmonic (λ_{exc} = 354.7 nm) of a Nd:YAG laser, operating at a frequency of 1 Hz.[16] To accomplish an homogeneous isomer distribution in the DS measurements by stirring, only one in every three shots was let through the shutter. A homemade variable delay box controlled the measurements. The excitation beam was shaped by a slit ($w \times h = 0.8 \times 6$ mm), resulting in an acoustic transit time of about 500 ns, allowing a time resolution down to ∼50 ns, employing deconvolution algorithms.[17] All samples were measured in a brass cuvette holder ensuring heat exchange through all four vertical walls, thus minimizing the temperature gradient in the cuvette to a maximum of ± 0.1 degrees. 100 shots (<10 μJ per shot) were averaged per signal trace and 2−8 traces were measured for each solution and temperature. Each DS sample received only 200 shots, corresponding to a total conversion < 1% in each isomerization direction, and was then replaced by another aliquot of the standard solution for further measurements.

Three series of LIOAS experiments were carried out. The first series performed in a temperature range 4−35 °C was restricted to NH_4^+ as the countercation, in view of the fact that the HPLC separation of the *cis* isomer was performed with an NH_4 CH_3COO aqueous solution as part of the mobile phase (vide supra). The second and third series included the different cations mentioned above for the *trans* to *cis* isomerization. The data obtained at only two close temperatures (the two-temperatures method, TT method, vide infra) were used in the two latter sets. The third series also included neat water (again only for the *trans* to *cis* isomerization), and the data were evaluated using deconvolution. In all three series, the isomerization quantum yield for both isomerization directions was determined.

The use of two close lying temperatures (TT method)[16,18] was favored in this case over the several temperatures method, in view of the fact that the results with the latter method showed deviations from linearity.

$O_2(^1\Delta_g)$ Quantum Yield, Φ_Δ. The $O_2(^1\Delta_g)$ quantum yield, Φ_Δ, was determined for the third series of experiments by monitoring the photoinduced luminescence at 1270 nm as already described,[19−21] with the same laser as described above. The beam was shaped by a 3 mm diameter pinhole and the repetition rate was 1 Hz. A liquid-nitrogen cooled germanium diode (EO-817P, North Coast) in combination with a silicon and an interference filter was used for detection.[21] Laser energies were 0.5 mJ per pulse for *trans*-DS and TSPP and 1 mJ for *cis*-DS. Data were recorded as in LIOAS, again averaging 100 shots per trace. A total of 6 traces was acquired per sample and reference, respectively. The DS samples were replaced after 100 shots.

Isomerization Quantum Yields. Isomerization quantum yields were determined at 6 °C, using the same optical conditions as for LIOAS. The total fluence absorbed by the sample was also measured as in LIOAS (vide supra). Excitation was at 1 Hz. After application of a defined total energy a UV−vis spectrum was taken. Thereafter, the sample was submitted to further irradiation. In these experiments the total conversion was always < 10%.

Fluorescence Quantum Yield. The fluorescence quantum yield was determined by comparison of the integrated emission spectra with that of a standard solution of quinine sulfate in 0.1 N sulfuric acid.[22]

Data Processing and Handling. Data processing was carried out with commercial PC software. LIOAS data were deconvoluted using Sound Analysis, Version 1.50D (Quantum Northwest Inc., Spokane, WA). All fittings were performed with Microcal

Origin Professional, Version 5.0 SR2 (Microcal Software, Inc., Northampton, MA). PM3 calculations were performed using Spartan, Version 4.0.4; Wave function: Irvine, 1995 (Hehre, W. J.; Huang, W. W.; Burke, L. D.; Shusterman, A. J.)

The amplitudes, φ_i, recovered from the deconvolution depend on $c_p\rho/\beta$, calculated for water from the values in tables.[23] Plotting φ_i vs $c_p\rho/\beta$ reveals a linear behavior with α_i, released in the step i, as intercept and the corresponding structural molar volume change, $\Delta V_{R,i}$, times the quantum yield, Φ_i, as slope[16,24,25]

$$\varphi_i = \alpha_i + \left(\frac{c_p\rho}{\beta}\right)_T \frac{\Phi_i \Delta V_{R,i}}{E_\lambda} \quad (1)$$

The introduction of a salt results in an alteration of $c_p\rho/\beta$. To determine this ratio, comparative measurements of the calorimetric references in the various cation solutions and in neat water were performed. The plot of the laser-energy normalized LIOAS amplitudes for the reference vs temperature (plots not shown) reflects the behavior of $\beta/(c_p\rho)$.[25,26] The main feature is obviously a far reaching parallelism between all curves, especially in the range 2.8−6.0 °C, i.e., in the temperature range in which the quantitative LIOAS experiments were carried out. Thus, in this relatively small range the salt addition only changes the transition temperatures ($\vartheta_{\beta=0}$, at which the thermal signal component vanishes), which were $\vartheta_{\beta=0} = 3.9$ °C for neat water and 3.2, 2.9, 3.1, 2.9, and 3.0 °C for $N(CH_3)_4^+$, Cs^+, NH_4^+, K^+, and Na^+ acetate aqueous solutions, respectively (all salts were 0.09 M).

Results

LIOAS. The data for the series including the various countercations and neat water for the *trans* to *cis* photoisomerization were analyzed with eq 2 using data at $\vartheta_{\beta=0}$ and at a second temperature, $\vartheta_{\beta\neq0}$, not far apart from $\vartheta_{\beta=0}$[18,16]

$$\alpha_i = \varphi_i(\vartheta_{\beta\neq0}) - \varphi_i(\vartheta_{\beta=0})$$

$$\Phi_i \Delta V_{R,i} = \varphi_i(\vartheta_{\beta=0}) \left[\frac{\beta}{c_p\rho}\right]_{\vartheta_{\beta\neq0}} E_\lambda \quad (2)$$

The individual points for the two-temperatures (TT) analysis were obtained by performing up to four times more averages (ca. 800 traces were averaged) than for the several-temperatures (ST) analysis. In every case, the deconvolution of these data revealed a two-components kinetics. In addition to the prompt component ($i = 1$, $\tau_1 < 20$ ns), a second one could be detected ($i = 2$) with a lifetime of ca. 75 ns (the exact value depending of the particular measurement) in the air-saturated solutions.

Figure 1 shows the LIOAS data for *trans*- and *cis*-DS in NH_4CH_3COO solution (at $\vartheta_{\beta\neq0} = 5.5$ °C) together with that for the respective reference, the simulated curve, and the residuals. The curves for the stilbenes at $\vartheta_{\beta=0}$ are also included. The deconvolution results for all samples are summarized in Table 1.

In the first and second series with *trans*- and *cis*-DS there was no indication of any resolvable kinetics. In this special case, no deconvolution is necessary, and it is sufficient to use the energy-normalized signal amplitude, H_n. Under these circumstances, φ_i in eqs 1 and 2 is simply replaced by the quotient H_n^{sam}/H_n^{ref}.[2,3,26] For the data analysis $\vartheta_{\beta=0}$ and 5 °C were used. The results were $\Delta H_{tc} = (35 \pm 35)$ kJ/mol and $\Delta V_{tc} = -(1.1 \pm 0.15)$ ml/mol.

Isomerization Quantum Yields. The isomerization quantum yields were determined from absorption changes following irradiation. The molar absorption coefficient for *trans*-DS determined with solutions containing weighted amounts of the compound resulted to be $\epsilon_t = (26400 \pm 1800)$ $M^{-1}cm^{-1}$ at 355 nm. The normalization of the *cis* spectrum was done with the absorption coefficient of the *trans* spectrum at the isosbestic point, $\lambda_{isosb} = (311.2 \pm 0.2)$ nm. The calculated value for the *cis* isomer at 355 nm was $\epsilon_c = (5900 \pm 600)$ $M^{-1}cm^{-1}$.

The *trans*- and *cis*-DS samples were irradiated stepwise for the determination of the isomerization quantum yields, $\Phi_{t\rightarrow c}$ and $\Phi_{c\rightarrow t}$. After the application of defined photon fluxes, the induced changes in the absorption spectra were recorded and fitted with the spectra of the pure isomers. The inset in Figure 2 shows such a mixed spectrum as well as the contributing isomer spectra. From the fits the concentrations of the individual isomers were determined and inserted into eq 3[27]

$$\Psi = \left(1 + \frac{A'}{2} + \frac{A'^2}{12}\right) \ln\left(\frac{[trans]_0}{[trans]}\right) + \frac{3 + A'}{6}(\epsilon'_t - \epsilon'_c)[cis]d + \ldots + \frac{1}{24}(\epsilon'_t - \epsilon'_c)^2 d^2 (2[trans]_0[cis] - [cis]^2) \quad (3)$$

$$= \frac{\Phi_{t\rightarrow c} d\epsilon'_t}{V} n_{phot}$$

$$A' = \epsilon'_c\, d[trans]_0,\ \epsilon' = 2.3\epsilon^{355}$$

This equation (eq 3) is written for the photoisomerization direction *trans* → *cis* and takes into account absorption changes upon irradiation. d is the optical path length, $[trans]_0$ is the initial concentration, V is the solution volume, and n_{phot} is the incident photon amount.

The slope of the plot of Ψ vs n_{phot} for both isomerization directions (Figure 2) yields the respective quantum yield, $\Phi_{c\rightarrow t} = 0.27 \pm 0.08$ and $\Phi_{t\rightarrow c} = 0.47 \pm 0.08$. $\Phi_{t\rightarrow c}$ is the average of a series in 90 mM aqueous NH_4CH_3COO solution and another one in neat water. Both series afforded the same result within the error limits.

$\Phi_{t\rightarrow c}$ was not altered by the various cations as verified by comparing the spectra before and after the application of a defined photon flux. Because the shape of the corresponding spectra was always the same it was enough to monitor the absorbance changes at one particular wavelength (350 nm). The initial absorbance at 350 nm was always $A^{350} = 0.300 \pm 0.005$. The absorption changes plotted vs the incident photon quantity are depicted in Figure 3. For all solutions the points for similar photon fluxes are found within small "clouds" representing the error distribution. Thus, $\Phi_{t\rightarrow c}$ is the same within the error limits for all solutions.

Fluorescence Quantum Yields. The fluorescence quantum yields resulted to be $< 10^{-2}$ for both DS isomers.

Determination of Φ_Δ. The determination of Φ_Δ was performed by comparing the near-IR emission upon photoexcitation of aerated solutons of *trans*- and *cis*-DS with that of an aerated solution of TSPP in tris buffer (pH = 7.8) with $\Phi_\Delta = 0.62 \pm 0.05$.[28]

No near-IR luminescence signals were observed for *trans*- and *cis*-DS in NH_4CH_3COO, although rather high energies were applied (about 26 photons per *trans*-molecule and 12 photons per *cis*-molecule initially present). From the amplitude of the TSPP signal it is concluded that $\Phi_\Delta \leq 0.05$ for both isomers.

The small $\Phi_\Delta \leq 0.05$ is mainly due to kinetic reasons, considering that DS triplet state is simply too short-lived to generate $O_2(^1\Delta_g)$ by quenching in aqueous solutions. Assuming a diffusion-controlled quenching obeying spin statistics, a maximum $O_2(^1\Delta_g)$ generation rate of $R_\Delta = 1/9\ k_0\ [O_2]$ is expected.[29] With $k_0 = 1.2 \times 10^{10}$ $M^{-1}s^{-1}$ estimated with the

TABLE 1: Data Derived from the Deconvolution of the LIOAS Signals (e.g., Figure 2) for the Triplet State Production (Subindex 1, eq 2) and Decay (Subindex 2, eq 2) of DS in Aqueous Solutions of Various Cations and in Neat Water[a]

	trans → *cis*						*cis* → *trans*
	H_2O	$N(CH_3)_4^+$	Cs^+	NH_4^+	K^+	Na^+	NH_4^+
	fast component (triplet production)						
$\Phi_1\Delta V_{R,1}$ (ml/mol) (τ_1<20ns)	−1.28 (± 0.05)	−0.81 (± 0.05)	−0.90 (± 0.05)	−1.03 (± 0.10)	−1.02 (± 0.10)	−1.04 (± 0.05)	−0.19 (± 0.10)
α_1	0.65 (± 0.10)	0.53 (± 0.10)	0.52 (± 0.10)	0.54 (± 0.10)	0.61 (± 0.10)	0.56 (± 0.10)	0.42 (± 0.15)
	slow component (triplet decay)						
$\Phi_2\Delta V_{R,2}$ ($\tau 2$ = 75 ns ± 20 ns)	0.52 (± 0.05)	0.17 (± 0.05)	0.34 (± 0.05)	0.44 (± 0.10)	0.45 (± 0.10)	0.35 (± 0.05)	0.54 (± 0.10)
α_2	0.37 (± 0.10)	0.45 (± 0.10)	0.38 (± 0.10)	0.42 (± 0.10)	0.38 (± 0.10)	0.44 (± 0.10)	0.63 (± 0.15)

[a] The two temperature analysis was applied.

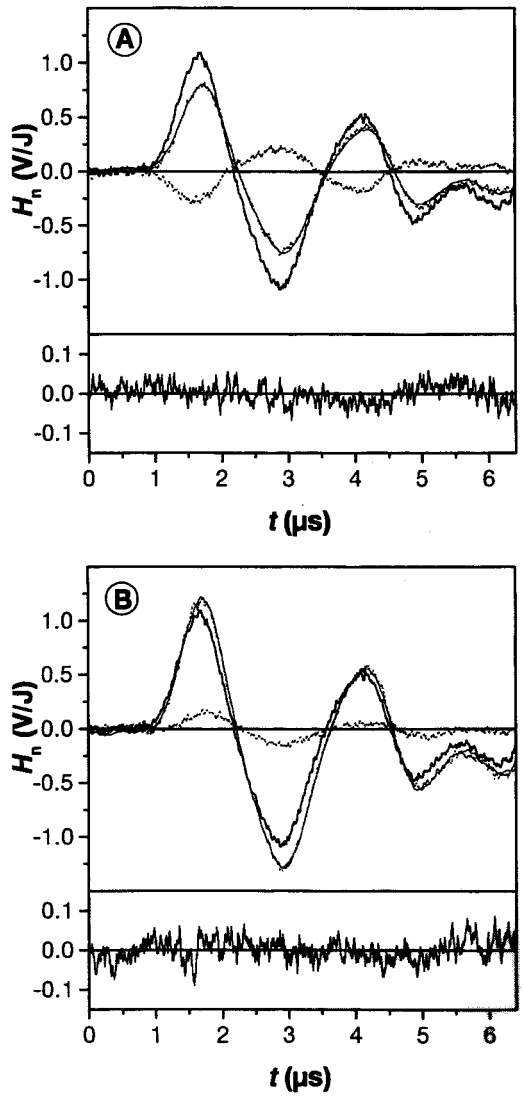

Figure 1. LIOAS signals at 5.5 °C in aerated aqueous 90 mM NH_4-CH_3COO solution (dotted lines) for (**A**) *trans*-DS, τ_1 < 20 ns, φ_1 = 0.15 ± 0.11; τ_2 = (75 ± 20) ns, φ_2 = 0.59 ± 0.11, and (**B**) *cis*-DS, τ_1 < 20 ns, φ_1 = 0.35 ± 0.15; τ_2 = (75 ± 20) ns, φ_2 = 0.84 ± 0.15, together with the respective reference (thick solid line), the simulated curve (fine solid line), and the residuals of the fitting. In both panels, the smallest signals (dashed line) are for the corresponding DS isomer at $\vartheta_{\beta=0}$ = 3.1 °C. The reference solution shows a zero signal at $\vartheta_{\beta=0}$.

Smoluchowski equation and $[O_2]$ in aerated water,[30] a maximum R_Δ value of ca. 3.3×10^6 s^{-1} is calculated. Compared to the decay rate of $k_T = 1/(75\text{ ns}) = 1.3 \times 10^7$ s^{-1}, triplet quenching by O_2 can only contribute to T decay with ca. 3%, that is, the expected value is in good agreement with the experimental value

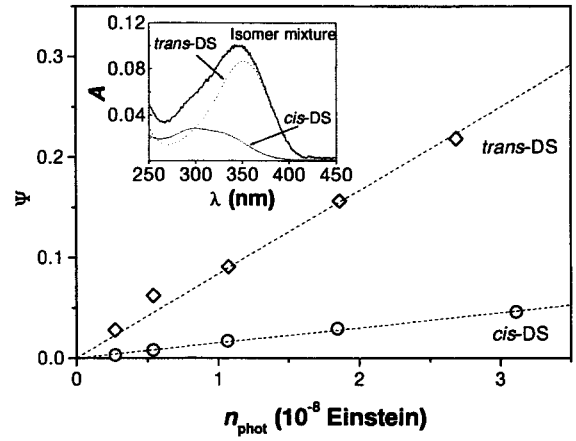

Figure 2. Ψ vs n_{phot} for both isomerization directions at 5 °C. The slopes yield the respective quantum yields, $\Phi_{t\rightarrow c}$ and $\Phi_{c\rightarrow t}$, according to eq 3. The inset shows a mixture spectrum as well as the contributing isomer spectra.

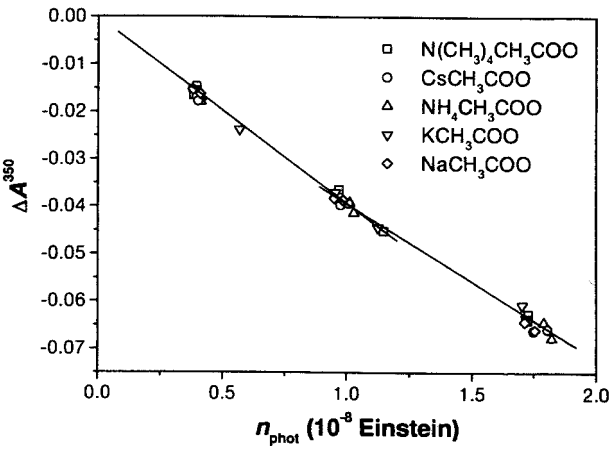

Figure 3. Absorption changes at 350 nm, $\Delta A,^{350}$ of *trans*-DS in the various aqueous solutions of monovalent salts, vs the incident photon quantity. The initial absorbance was always A^{350} = 0.300 ± 0.005.

of $\Phi_\Delta \leq 0.05$ in aerated aqueous DS solutions. Similar to the present case, relatively low Φ_Δ values have been reported for *trans*-4,4′-dinitrostilbene in organic solvents, despite the high intersystem crossing quantum yield.[31]

Discussion

The data obtained during the third series of experiments for the two components of the LIOAS signal deconvolution after excitation of *trans*- and *cis*-DS are collected in Table 1. The quantum yields are necessary to determine ΔV_i and ΔH_i from these data. Görner and Kuhn[14] discussed the photoisomerization mechanism for nitrostilbenes, depicted in Figure 4. The intro-

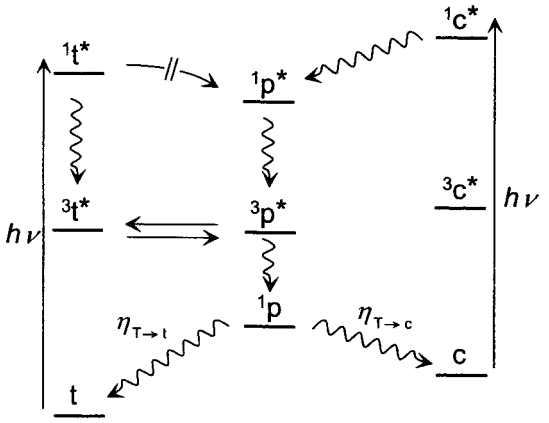

Figure 4. Isomerization mechanism for nitrostilbenes.[14,31−33] A thermally equilibrated mixture (T) of the lowest *trans* triplet state, ^{3}t*, and the lowest perpendicular triplet state, ^{3}p*, is formed. This figure was adapted from Görner and Kuhn (Scheme 3).[14]

duction of nitro groups strongly enhances intersystem crossing and isomerization upon excitation of *trans*-4,4′-dinitrostilbene occurs 100% from the triplet state.[32] For DS in aqueous solution, we have assumed that also from the *cis* isomer the photoisomerization involves mostly the triplet state. Thus, photoisomerization in both directions implies the triplet state mixture, T, i.e., a thermal equilibrium is established between the lowest *trans* triplet, ^{3}t*, and the triplet of the perpendicular state, ^{3}p*.[32,33] According to Görner and Kuhn[14] the rate constant for the step $^3p^* \rightarrow {}^1p$ is $(1-3)\times 10^7 s^{-1}$ (in organic solvents at room temperature). Hence, the quantum yields for the first step (establishment of the triplet equilibrium) and for the total process (including the decay to the ground state of either the *cis*- or the *trans*-isomer) are different. Using the decay efficiency from T to *cis* ($\eta_{T\rightarrow c}$) and T to *trans* ($\eta_{T\rightarrow t}$) with $\eta_{T\rightarrow c} + \eta_{T\rightarrow t} = 1$, the products of quantum yields and structural volume changes for the individual steps can be written as in eq 4. The subscripts, t and c, indicate which isomer was excited

$$(\Phi_1 \Delta V_{R,1})_t = \Phi_{t\rightarrow T} \Delta V_{tT}$$

$$(\Phi_2 \Delta V_{R,2})_t = \Phi_{t\rightarrow T}(\eta_{T\rightarrow c} \Delta V_{Tc} + \eta_{T\rightarrow t} \Delta V_{Tt}) \qquad (4)$$

$\Phi_{t\rightarrow T}$ and $\Phi_{c\rightarrow T}$ are the quantum yields for the formation of T coming from the *trans* and the *cis* side, respectively. The first component ($\tau_1 < 20$ ns) is the production of T, whereas the second component (with a lifetime τ_2 and associated with Φ_2 ΔV_2) comprises the changes upon T decay to *trans* and to *cis* ground-state DS, with efficiencies $\eta_{T\rightarrow c}$ and $\eta_{T\rightarrow t}$, respectively.

In general terms, ΔV_{AB} is the structural volume change on going from state A to state B (the same notation is used for the enthalpies) and $\Delta V_{AB} = -\Delta V_{BA}$.

On the other hand, eq 5 holds for the overall quantum yield

$$\Phi_{t\rightarrow c} \Delta V_{tc} = (\Phi_1 \Delta V_{R,1})_t + (\Phi_2 \Delta V_{R,2})_t \qquad (5)$$

The eqs 4 and 5 are written for the *trans* to *cis* direction. They can readily be changed for the opposite direction by interchanging the indices t and c.

According to eq 4, $\Phi_2 \Delta V_{R,2}$ obtained by excitation of *trans*- and *cis*-DS, respectively, contains information on the formation quantum yields of T in a manner that the ratio of these two terms gives the ratio of the respective quantum yields. The same holds of course also for the ratio of the corresponding released heat, α_2

$$\frac{\Phi_{t\rightarrow T}}{\Phi_{c\rightarrow T}} = \frac{(\Phi_2 \Delta V_{R,2})_t}{(\Phi_2 \Delta V_{R,2})_c} = \frac{(\alpha_2)_t}{(\alpha_2)_c} \qquad (6)$$

Combination of eqs 4, 5, and 6 gives access to the efficiencies of T decay ($\eta_{T\rightarrow c}$ and $\eta_{T\rightarrow t}$) and, thus, to the triplet formation quantum yields because $\Phi_{t\rightarrow c} = \Phi_{t\rightarrow T}\, \eta_{T\rightarrow c}$ and $\Phi_{c\rightarrow t} = \Phi_{c\rightarrow T}$ $\eta_{T\rightarrow t}$. This calculation was possible because the isomerization of DS could be measured in both directions (albeit under restricted conditions for the *cis* isomer).

A prerequisite for the calculation is that there is no other pathway of triplet deactivation, i.e., $O_2(^1\Delta_g)$ is not generated, as was effectively shown.

A similar situation as for the structural volume change exists for the energy release. The enthalpy difference between the two isomers (ΔH_{tc}) and between these isomers and the triplet state (ΔH_{tT} and ΔH_{cT}) are derived using energy balance considerations from the values α_i and the quantum yields according to eq 7 again written for the *trans* → *cis* direction

$$\Delta H_{tT} = \frac{1}{\Phi_{t\rightarrow T}}(1 - (\alpha_1)_t)\, E_\lambda$$

$$\Delta H_{tc} = \frac{1}{\Phi_{t\rightarrow c}}(1 - [(\alpha_1)_t + (\alpha_2)_t])\, E_\lambda \qquad (7)$$

The set of eqs 4−7 allows to transform the data in Table 1 to the molar quantities summarized in Table 2.

The plot of the energy differences between the individual isomers and the triplet state vs the structural molecular volume change is shown in Figure 5A. The squares are for the *trans* → *cis* direction (first six columns in Table 2) and the circles for *cis* → *trans* (Table 2, last column). The filled symbols represent the step from the initial isomer toward the triplet state (Table 2, upper panel) and the open symbols indicate the step from the triplet state toward the respective opposite isomer (Table 2, middle panel). For this reason, a central symmetry with respect to the origin of the plot is found between points for the two directions.

The energy of both isomers lies about 200 kJ/mol below the triplet state [$\Delta H_{cT} = (199 \pm 50)$ kJ/mol and $\Delta H_{tT} = (215 \pm 38)$ kJ/mol], in good agreement with the values obtained from the PM3 calculation ($\Delta H_{cT} = 133$ kJ/mol and $\Delta H_{tT} = 170$ kJ/mol, vide infra).

The most significant difference between the *trans* and *cis* isomers is the change in molecular volume upon going to the triplet state. The transition *trans* → T is associated with a contraction of $\Delta V_{tT} = -(1.4 \pm 0.15)$ ml/mol. A smaller contraction of $\Delta V_{cT} = -(0.15 \pm 0.15)$ ml/mol is found for the *cis* → T step. The values for both the enthalpy differences and the structural volume changes are averages of all available values, i.e., ΔH_{cT} and $-\Delta H_{Tc}$ as well as ΔV_{cT} and $-\Delta V_{Tc}$, and the corresponding values involving the *trans* isomer, in Table 2 for all solutions and both isomerization directions.

The corresponding plot for the overall process is shown in Figure 5B (Table 2, lower panel). The average values for the total process including all series are $\Delta V_{tc} = -(1.2 \pm 0.1)$ ml/mol and $\Delta H_{tc} = (28 \pm 35)$ kJ.

Neither for the individual resolvable steps nor for the total process, a systematic correlation between structural changes, enthalpy difference, and the cation present could be found. This finding was supported by the data from the series of measurements in which only the LIOAS amplitudes were used for the

TABLE 2: Molar Volume and Enthalpy Changes for the Triplet Production (Upper Panel), the Triplet Decay (Middle Panel), and the Total Process[a]

trans → *cis*						*cis* → *trans*
H_2O	$N(CH_3)_4^+$	Cs^+	NH_4^+	K^+	Na^+	NH_4^+
		$\eta_{T\rightarrow c} = 0.70 \pm 0.20$				$\eta_{T\rightarrow t} = 0.30 \pm 0.20$
		$\Phi_{t\rightarrow T} = 0.70 \pm 0.20$				$\Phi_{c\rightarrow T} = 0.85 \pm 0.50$
		ΔV_{tT} (ml/mol)				ΔV_{cT} (ml/mol)
−1.85 (± 0.55)	−1.15 (± 0.35)	−1.30 (± 0.40)	−1.50 (± 0.45)	−1.50 (± 0.45)	−1.50 (± 0.45)	−0.20 (± 0.20)
		ΔH_{tT} (kJ/mol)				ΔH_{cT} (kJ/mol)
170 (± 105)	230 (± 90)	235 (± 90)	225 (± 95)	190 (± 105)	215 (± 95)	230 (± 120)
		ΔV_{Tc} (ml/mol)				ΔV_{Tt} (ml/mol)
0.25 (± 0.55)	−0.20 (± 0.40)	0.10 (± 0.40)	0.25 (± 0.50)	0.25 (± 0.45)	0.05 (± 0.50)	1.50 (± 0.35)
		ΔH_{Tc} (kJ/mol)				ΔH_{Tt} (kJ/mol)
−185 (± 140)	−215 (± 130)	−165 (± 125)	−195 (± 130)	−185 (± 140)	−215 (± 135)	−260 (± 290)
		ΔV_{tc} (ml/mol)				ΔV_{ct} (ml/mol)
−1.60 (± 0.20)	−1.35 (± 0.15)	−1.20 (± 0.15)	−1.25 (± 0.15)	−1.20 (± 0.15)	−1.45 (± 0.20)	1.30 (± 0.30)
		ΔH_{tc} (kJ/mol)				ΔH_{ct} (kJ/mol)
−15 (± 95)	15 (± 95)	70 (± 90)	30 (± 95)	5 (± 95)	0 (± 95)	−30 (± 265)

[a] The data from Table 1 were processed using the quantum yields $\Phi_{t\rightarrow c}$ and $\Phi_{c\rightarrow t}$ (eq 3) and the efficiencies $\eta_{T\rightarrow c}$ and $\eta_{T\rightarrow t}$ (eqs 4 and 5).

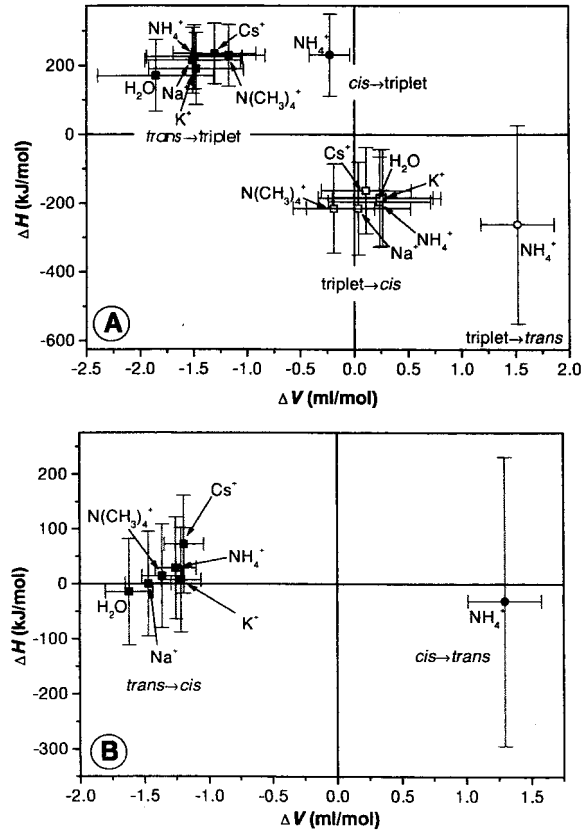

Figure 5. (**A**) Enthalpy difference, ΔH_{AB} between the individual isomers and the triplet state vs the structural molecular volume change, ΔV_{AB}. (■) ΔH_{tT} vs ΔV_{tT}, for the *trans* → T transition, (□) ΔH_{Tc} vs ΔV_{Tc}, for the T → *cis* transition, derived from the analysis of the 1st and 2nd component, respectively, of the LIOAS signal upon *trans*-DS excitation. (●) ΔH_{cT} vs ΔV_{cT}, for the *cis* → T transition, (○) ΔH_{Tt} vs ΔV_{Tt}, for the T → *trans*, from the LIOAS signal upon *cis*-DS excitation. (**B**) Enthalpy differences between the isomers vs. their molecular volume differences: (■) ΔH_{tc} vs ΔV_{tc}, for the isomerization *trans* → *cis*, (●) ΔH_{ct} vs ΔV_{ct}, for the isomerization *cis* → *trans*.

evaluation. In the corresponding figure (equivalent to Fig 5B, not shown) a randomly different distribution of the data points for the various cations was found for the *trans* → *cis* photoisomerization. Also, in this case, all points were in the "cloud" formed by the overlapping error bars. In addition, attempts to correlate enthalpy and volume changes (see ref 9) determined in the two series in which measurements were carried out with various cations, led to similar but unrealistic fit results. We attribute the false apparent correlation to error compensations.[34] These arguments strongly indicate that in this case no compensation effect between ΔH and ΔV is observed, in contrast to previous findings for other systems.[9]

The most important feature of the isomerization process for both *cis*- and *trans*-DS is that the triplet production is always linked to a contraction (cf. the values quoted above), whereas the triplet decay always results in an expansion.

To understand the origin of this behavior the electrostatic interaction resulting in electrostriction between DS and the solvent molecules was calculated.[1,4,7,35,36] Within the frame of the electrostriction theory, the molecule is regarded as a hard sphere interacting with the solvent assumed to be a continuum of dielectric constant ϵ. This treatment leads to the Drude−Nernst equation originally developed for purely Coulombic (monopole) interactions[4]

$$\Delta V_{elect} = \frac{1}{2}\frac{(ze)^2}{r}\frac{\partial(\epsilon^{-1})}{\partial p} = -B\frac{z^2}{r} \qquad (8)$$

z is the charge, r is the molecule radius, and p is the pressure. This equation can easily be converted into eq 9 for the case of dipole interactions[37]

$$\Delta V^{\mu}_{elect} = \frac{3}{4}\frac{\mu^2}{r^3}\frac{\partial(\epsilon^{-1})}{\partial p} \qquad (9)$$

with μ the dipole moment. The Drude−Nernst equation can be transformed using the Clausius−Mossotti equation to circumvent the use of $\partial(\epsilon^{-1})/\partial p$ for which not many reliable values can be found in the literature.[5,7] However, the Clausius−Mossotti equation is only valid for non polar solvents. For polar solvents the underlying model does not hold inasmuch as compression of the regarded molecule also plays a role. Taking this into account, eq 10 is obtained upon expanding the electrostriction

TABLE 3: Total Binding Energy, H^0, Dipole Moment, μ, and C7−C8 Bond Length, l, Calculated Using the PM3 Semiempirical Method

	trans-DS	DS in perpendicular triplet state	*cis*-DS
H^0 (kJ/mol)	−1065	−895	−1028
μ (D)	0.05	4.08	4.11
l (Å)	1.343	1.434[a]	1.335

[a] The bond length, l, for the perpendicular state is not comparable in the sense that there is no double bond in this case.

considerations to the dipole interaction[37]

$$\Delta V_{\text{elect}} = \frac{1}{2}\frac{z^2e^2}{r}\left(\frac{\partial(\epsilon^{-1})}{\partial p} + \frac{\partial(\ln r)}{\partial p}\right) + \frac{3}{2}\frac{\mu^2}{r^3}\left(\frac{1}{2}\frac{\partial(\epsilon^{-1})}{\partial p} + \frac{\partial(\ln r)}{\partial p}\right) \quad (10)$$

The first term in parentheses of the sum in eq 10 reflects Coulombic interactions, the second is due to dipole interactions. Terms of higher order are neglected here. $\partial(\epsilon^{-1})/\partial p$ refers to the solvent effects and $\partial(\ln r)/\partial p$ describes changes in molecular size due to the force exerted on the molecule by the solvent.

The complex structure of eq 10 is reflected in the fact that the value calculated in water with eq 8 (B = 4.175 Å ml/mol) must be replaced by a significantly higher semiempirical value, $B_{emp} = (9.6 \pm 1.5)$ Å ml/mol,[35,36] that is, the measured volumes are due not only to solvent reorganization without a volume change of the molecule itself (very first term in eq 10).

Notwithstanding the above problems, a rough estimation of the electrostriction was made by assuming B_{emp} to be valid for our system in order to calculate $\partial(\ln r)/\partial p$ with eq 10. The dipole term in eq 10 is the appropriate term to describe the electrostriction volume changes upon a change in the dipole moment. This term is very sensitive to the molecular radius, r. A spherical molecule was assumed which is justified for *cis*-DS ($r \approx 6$ Å) but not for *trans*-DS where a cylindrical shape (14 Å × 10 Å) is found. Thus, $\Delta V^{\mu}_{\text{elect}}$ was calculated not only with $r = 6$ Å, but also with 3 Å. Using the calculated value $\mu = 4$ D (cf. Table 3) as well as the approximation $r \approx 6$ Å, a volume change due to electrostriction of ca.-0.1 mL/mol is obtained for the *trans* → *cis* transformation. With the extreme value of $r = 3$ Å (as a minimum value in view of the flat form of the *trans* cylinder) and the upper error limit of B_{emp}, however, an upper limit of $|\Delta V^{\mu}_{\text{elect}}| \leq 0.7$ ml/mol is obtained. It is clear that the empirical value B_{emp} should also contain specific interactions between the molecule and its solvent environment, e.g., H-bridges. However, the volume changes calculated with B_{emp}, are not big enough to explain the molar values of ΔV_{AB} for DS even if B_{emp} reflects such interactions.

Whatever the quantitative explanation for the value of the structural volume change is, should specific stilbene-water interactions be responsible for the observed effects, changes in the water structure would affect the results.[9,38] However, the experiments in the presence of monovalent cations (of organizing and unorganizing nature) yield all, within the error limits, the same results as those of the experiment with *trans*-DS in neat water (Figure 5). Although in the solutions with added salt the DS anions (always at ca. 10^{-5} M) should be mostly surrounded by the countercations, no influence of the nature of the cation upon photoisomerization was detected. These results indicate that the contraction observed should be mainly attributed to intrinsic effects, as it was the case with the $Ru(bpy)_3^{+2}$ cation in water.[9]

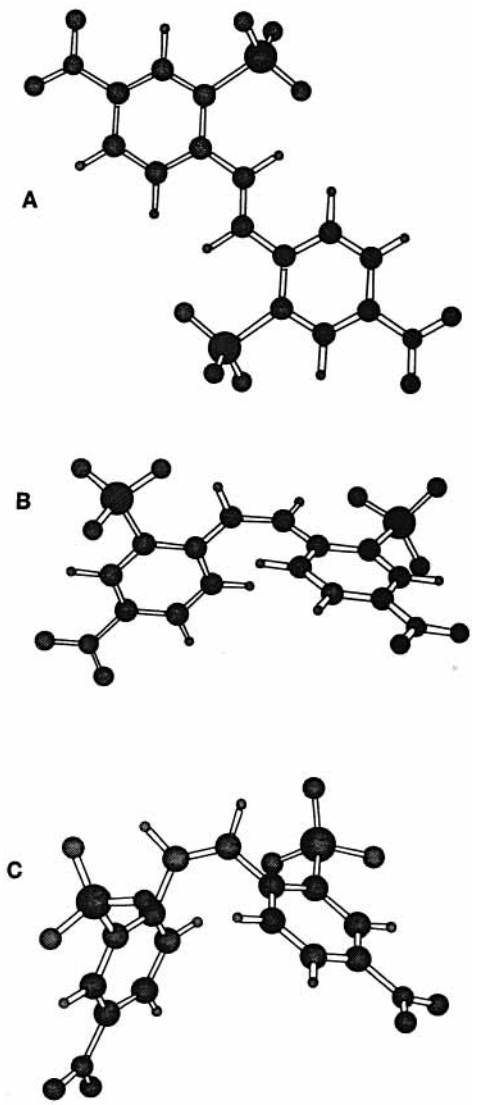

Figure 6. PM3 optimized geometries for (**A**) *trans*-DS, (**B**) DS in its perpendicular triplet state, and (**C**) *cis*-DS.

Contrary to the large expected shortening of the Ru−N bonds in $Ru(bpy)_3^{+2}$ upon photoexcitation, only a small shortening of the C═C bond was calculated for the *trans* → *cis* DS photoisomerization (Table 3). However, a rough calculation using the dimensions of both DS isomers, i.e., a cylinder for the *trans* and a sphere for the *cis* isomer, affords molecular volumes of 662 and 544 Å^3, respectively, pointing to a large contraction from *trans* to *cis*, although this is a very crude estimation which does not consider the accessibility of the water molecules. Therefore, we attribute at most 50% of the total structural volume change to electrostriction and the rest to an intrinsic volume change. Although very approximate, this picture explains the lack of effect of the salt variation as well as the sign of the observed effects.

Thus, the values obtained for the stepwise structural volume changes may be accounted for by analyzing the structure of the isomers and that of the intermediate state. The *trans* molecule possesses the largest intrinsic volume (and the highest conjugation). Hence, in this case, a loss in conjugation (as indicated by the somehow shorter C═C double bond in the *cis* isomer, Table 3) is concomitant with a decrease in volume leading to a contraction. A gain in conjugation, on the contrary, leads to an expansion. According to this line of arguments we should have observed much larger volume changes. The water accessibility,

larger for the *trans* than for the *cis* isomer, however, might compensate the effect to a certain degree.

The above arguments indicate that the states in equilibrium forming the intermediate T (the triplet perpendicular state ^{3}p*, devoid of conjugation of the C7−C8 bond, in equilibrium with the lowest *trans* triplet state ^{3}t*) have in average a structure more similar to the *cis* isomer than to the *trans* one because the contraction for the step *trans* → T is larger than that for the *cis* → T.

The only other determination of a structural volume change upon a stilbene isomerization known to us is that of the water insoluble *trans*-stilbene in mixtures of nonpolar solvents. The contribution of ΔV_R to the LIOAS signal could not be separated in these mixtures. An expansion of 5.6 mL/mol was reported for the *trans* → *cis* photoreaction in micellar solutions.[39] No results were reported for the *cis* → *trans* photoisomerization in this molecule. In view of the differences in photochemical mechanisms (the *trans*−*cis* photoisomerization in stilbene occurs through a singlet mechanism vs the triplet mechanism in the nitrostilbenes[14]), and the differences in media it makes no sense comparing our present data with those by Herman and Goodman.[39]

Regarding the enthalpy difference between both DS isomers, geometry optimization performed by PM3 calculations (cf. Table 3, and Figure 6)[40] indicate that the energy of *trans*-DS in the gas-phase lies 37 kJ/mol below that of *cis*-DS. This is in agreement with the experimental data, notwithstanding the large error, $\Delta H_{ct} = -(28 \pm 35)$ kJ/mol, vide supra. The comparison between the experimental and the calculated value is justified because the calculated change in dipole moment upon photoexcitation is very small and no big changes in the electrostatic interactions with the medium upon photoisomerization are expected (as shown by the calculations presented above).

Acknowledgment. We are indebted to Dr. Helmut Görner for many fruitful discussions, to Dr. Paul Verhoeven for preliminary molecular mechanics calculations, and to Professor Kurt Schaffner for his continuous support of this project. We are very grateful to Gul KoH-Weier for the separation of the DS isomers by HPLC and acknowledge the able technical assistance of Gudrun Klihm, Dagmar Lenk, and Sigrid Russell. Miguel Angel Rodríguez was a fellow of the Alexander von Humboldt Foundation (1998 and 2000) and Alessandro Feis was recipient of an EU fellowship (1995).

References and Notes

(1) Van Eldik, R.; Asano, T.; Le Noble, W. J. *Chem. Rev.* **1989**, *89*, 549−688.

(2) Braslavsky, S. E.; Heibel, G. E. *Chem. Rev.* **1992**, *92*, 1381−1410.

(3) Churio, M. S.; Angermund, K. P.; Braslavsky, S. E. *J. Phys. Chem.* **1994**, *98*, 1776−1782.

(4) Drude, P.; Nernst, W. *Z. Phys. Chem.* **1884**, *15*, 79−85.

(5) Muñoz, R. C.; Holroyd, R. A.; Itoh, K.; Nagakawa, K.; Nishikawa, M.; Fueki, K. *J. Phys. Chem.* **1987**, *91*, 4639−4643.

(6) Rodríguez, M. A.; Braslavsky, S. E. *J. Phys. Chem. A* **1999**, *103*, 6295−6300.

(7) Wegewijs, B.; Verhoeven, J. W.; Braslavsky, S. E. *J. Phys. Chem.* **1996**, *100*, 8890−8894.

(8) Wegewijs, B.; Paddon-Row: M. N.; Braslavsky, S. E. *J. Phys. Chem. A* **1998**, *102*, 8812−8818.

(9) Borsarelli, C. D.; Braslavsky, S. E. *J. Phys. Chem. B* **1998**, *102*, 6231−6238 and references therein.

(10) Schulenberg, P. J.; Braslavsky, S. E. In *Progress in Photothermal and Photoacoustic Science and Technology*; Mandelis, A.; Hess, P., Eds.; SPIE: Bellingham, WA, 1997; pp 57−81.

(11) Gensch, T.; Hellingwerf, K. J.; Braslavsky, S. E.; Schaffner, K. *J. Phys. Chem. A* **1998**, *102*, 5398−5405.

(12) Losi, A.; Wegener, A. A.; Engelhard, M.; Gärtner, W.; Braslavsky, S. E. *Biophys. J.* **2000**, *78*, 2581−2589.

(13) Feis, A.; Wegewijs, B.; Gärtner, W.; Braslavsky, S. E. *J. Phys. Chem. B* **1997**, *101*, 7620−7627.

(14) Görner, H.; Kuhn, H. J. *Adv. Photochem.* **1995**, *19*, 1−117 and references therein.

(15) Saltiel, J.; Sun, Y.-P. In *Photochromism, Molecules and Systems*; Dürr, H.; Bouas-Laurent, H.; Elsevier: Amsterdam, 1990; pp 64−164.

(16) Losi, A.; Braslavsky, S. E.; Gärtner, W.; Spudich, J. L. *Biophys. J.* **1999**, *76*, 2183-2191.

(17) Rudzki-Small, J. E.; Goodman, J. L.; Peters, K. S. *J. Am. Chem. Soc.* **1985**, *107*, 7849−7854.

(18) Gensch, T.; Braslavsky, S. E. *J. Phys. Chem. B* **1997**, *101*, 101−108.

(19) Nonell, S.; Aramendía P. F.; Heihoff, K.; Negri, R. M.; Braslavsky, S. E. *J. Phys. Chem.* **1990**, *94*, 5879−5883.

(20) Mártire, D. O.; Jux, N.; Aramendía, P. F.; Negri, R. M.; Lex, J.; Braslavsky, S. E.; Schaffner, K.; Vogel, E. *J. Am. Chem. Soc.* **1992**, *114*, 9969−9978.

(21) Braslavsky, S. E.; Müller, M.; Mártire, D. O.; Pörting, S.; Bertolotti, S. G.; Chakravorti, S.; Koç-Weier, G.; Knipp, B.; Schaffner, K. *J. Photochem. Photobiol. B: Biol.* **1997**, *40*, 191−198.

(22) Eaton, D. F. *Pure Appl. Chem.* **1988**, *60*, 1107−1114.

(23) Weast, R. C. *CRC−Handbook of Chemistry and Physics*, 67thed.; CRC Press: Boca Raton, Fl, 1986.

(24) Rudzki-Small, J. E.; Libertini, L. J.; Small, E. W. *Biophys. Chem.* **1992**, *42*, 29−48.

(25) Crippa, P. R.; Vecli, A.; Viappiani, C. *J. Photochem. Photobiol. B*: *Biol.* **1994**, *24*, 3−15.

(26) Gensch, T.; Viappiani, C.; Braslavsky S. E. In *Encyclopedia of Spectroscopy and Spectrometry*, Tranter, G. E.; Holmes, J. L., Eds; Academic Press: San Diego, 1999; pp 1124−1132.

(27) Kropf, A.; Hubbard, R. *Photochem. Photobiol.* **1970**, *12*, 249−260.

(28) Gensch, T.; Viappiani, C.; Braslavsky, S. E. *J. Am. Chem. Soc.* **1999**, *121*, 10 573−10 582.

(29) Nau, W. M.; Scaiano, J. C. *J. Phys. Chem.* **1996**, *100*, 11 360−11 367, and references therein.

(30) Murov, S. L.; Carmichael, I.; Hug, G. L. *Handbook of Photochemistry*, 2nd ed.; Marcel Dekker: New York, 1993; p 207.

(31) Görner, H. *Ber. Bunsen-Ges. Phys. Chem.* **1998**, 102, 726.

(32) Görner, H. *Ber. Bunsen-Ges. Phys. Chem.* **1984**, *88*, 1199.

(33) Kuhn, H. J.; Straatmann, R.; Schulte-Frohlinde, D. *J. C. S. Chem. Commun.* **1976**, 824−825.

(34) Krug, R. R.; Hunter, W. G.; Grieger, R. A. *J. Phys. Chem.* **1976**, *80*, 2335−2340.

(35) Borsarelli, C. D.; Braslavsky, S. E. *J. Photochem. Photobiol. B* **1998**, *43*, 222−228.

(36) Millero, F. *Chem. Rev.* **1971**, *71*, 147−176.

(37) Whalley, E. *J. Chem. Phys.* **1962**, *38*, 1400−1405.

(38) Borsarelli, C. D.; Braslavsky, S. E. *J. Phys. Chem. A* **1999**, *103*, 1719−1727.

(39) Herman, M. S.; Goodman, J. L. *J. Am. Chem. Soc.* **1989**, *111*, 1849−1854.

(40) Stewart, J. J. P. *J. Comput. Chem.* **1989**, *10*, 209−220.